TABLE II. Values of $g'$ for ellipsoidal sample of Fe obtained for various different runs.

| Magnetizing current milliamps | | $g'$ |
|---|---|---|
| 4.00 | | 1.916 |
| 10.00 | | 1.918 |
| 5.00 | | 1.913 |
| 10.00 | | 1.920 |
| 5.00 | | 1.920 |
| 10.00 | | 1.918 |
| 10.00 | | 1.924 |
| 5.00 | | 1.921 |
| | Average | 1.919 |

pure iron was conducted at this new laboratory. In order to obtain uniform magnetization of the material, this sample was made in the form of a prolate spheroid. It had an eccentricity of 14.2 and was symmetrically placed in a hollow cylindrical winding which formed part of the torsional pendulum. Table I gives a list of the principal impurities in the sample. Table II shows a summary of this series of experiments which resulted in a $g'$ value for Fe of 1.919.

Readings were also taken on the cylindrical Fe specimen used in our earlier experiments.[4] These new readings resulted in a $g'$ value of 1.917.

TABLE III. Results of various $g'$ experiments on same sample of Ni.

| Reference | | $g'$ |
|---|---|---|
| a | | 1.837 |
| b | | 1.831 |
| b | | 1.834 |
| Present work | | 1.837 |
| | Average | 1.835 |

[a] S. Brown, A. J.-P. Myer, and G. G. Scott, Compt. rend. 238, 2504 (1954).
[b] See reference 5.

New experiments were also conducted on our old cylindrical specimen of Ni. Table III summarizes all of the values of $g'$ which have been measured for this sample of Ni excluding those obtained at low magnetization earlier.[5]

It is concluded from this work that $g'$ values should be 1.919±0.002 for Fe and 1.835±0.002 for Ni.

### ACKNOWLEDGMENTS

---

# Activation Energy for the Surface Migration of Tungsten in the Presence of a High-Electric Field*†

PHILIP C. BETTLER AND FRANCIS M. CHARBONNIER
*Linfield Research Institute, McMinnville, Oregon*
(Received February 5, 1960; revised manuscript received April 4, 1960)

An activation energy for the surface migration of tungsten atoms on the tungsten crystal lattice structure and under the influence of a high electric field has been measured using field emission techniques. The initially hemispherical field emitter tip surface deforms into a polyhedral shape in a process known as build-up, when the emitter is heated in the presence of large electrostatic forces. Build-up proceeds in a regular and reproducible manner; certain stages of build-up can be identified by characteristic changes in both the field emission patterns and the current vs time characteristics of the emitter. An activation energy of 2.44±0.05 ev/atom was determined, from the measured values of the time required to achieve a given degree of build-up at various operating temperatures. This value may be compared with the value of 3.14 ev/atom determined from the rate at which the tip of a heated tungsten emitter recedes in the absence of an electric field. Explanations for the difference are presented, involving two distinct factors: (1) a reduction in activation energy, through the effect of polarization of the surface atoms by the electrostatic field, by an amount which was determined in a special experiment; and (2) an inherent difference which remains after allowance has been made for the field effect. The latter is ascribed to the difference in the paths of migration in the two cases whereby, for the conditions existing in this experiment, the activation energy measured is that corresponding to migration primarily over the low index (100), (110), and (211) planes. A value of 2.79±0.08 ev/atom is obtained after correction for the field effect.

## I. INTRODUCTION

FIELD emission microscope techniques have yielded important advances in the understanding and measurement of surface migration. Two basic methods have been applied to quantitative migration studies:

(1) In the first method, the surface migration constants of selected adsorbates on a fixed substrate have been obtained from measurements of the surface rate of flow of such adsorbates whose presence alters the work function of the emitting surface and thus contributes changes in the emission which can be followed on the field emission pattern.[1,2]

[1] J. A. Becker, Advances in Catalysis 7, 135 (1955).
[2] Robert Gomer, Advances in Catalysis 7, 93 (1955).

(2) In the second method, which was used in the experiments described here, the self-migration constants for surface atoms on their own lattice are obtained from measurement of the time rate of change of the field emitter geometry, and the corresponding changes in the electron emission characteristics.

When no electric field is applied at the surface of the heated emitter, surface migration is caused by surface tension forces which produce a rounding and smoothing of the emitter tip and lead to subsequent dulling of the tip through a transport of material from the apex toward the shank. The activation energy of tungsten for the dulling process has been determined by Muller,[3] Dyke and co-workers,[4-6] and more recently by Sokolskaya.[7] Except for Muller's early values, the results are in good agreement and yield a value of approximately $Q_0 = 3.14$ ev/atom.

When a sufficiently high field is applied the electrostatic field forces predominate and reverse the direction of the migration, resulting in a geometric deformation of the emitter tip called "build-up" in which certain crystal planes become enlarged. The activation energy for build-up has been measured by Sokolskaya[7] and in the present work. Here again the results are in close agreement and yield a value of approximately $Q_F = 2.4$ ev/atom.

The difference between the values of $Q_0$ and $Q_F$ is well outside the respective experimental uncertainties. An explanation of this difference is proposed in the concluding section.

## II. THEORETICAL CONSIDERATIONS

The theoretical basis for the interpretation of the experimental data is found essentially in Herring's application of thermodynamic principles to the theoretical study of transport phenomena and of the associated geometrical changes in heated metal crystals.[8,9] This study yields a condition for the geometrical equilibrium of the solid-vacuum interface at the surface of an isothermal single crystal of arbitrary shape, and also gives an expression for the flux of atoms in the absence of equlibrium.

The field emitters used in the present experiments have, prior to build-up, a shape illustrated by the electron microscope shadowgraph of Fig. 8(a), i.e., they consist of a spherical tip smoothly fitted into a conical

shank. The emitter tip radius (normally less than one micron) is much smaller than average crystal dimensions in the tungsten emitter, so that the fraction of the emitter which is of primary interest in the build-up process normally consists of a single crystal to which Herring's theory may be applied. The experimental verification of Herring's theory through the study of heated field cathodes has been described in recent publications.[6,10,11] Scaling laws have been used to establish that surface migration is the transport process predominantly responsible for the geometrical changes observed in heated field emitters. Surface tension, and surface stress gradients produced by application of an electric field at the emitter surface, supply the motivating forces responsible for the migration.

Surface tension forces predominate at low values of the applied electric field, resulting in a net migration of atoms away from the tip which causes the heated emitter tip to recede and dull with time; experimental measurement of the receding rate as a function of applied field yields a determination of the surface tension $\gamma$ and the surface migration constants for the emitter material.[6]

For intermediate values of the applied field a balance can be achieved between surface tension and electrostatic forces, whereby the net surface migration rate is essentially reduced to zero and geometrical stability of the heated surface is maintained. This case is of great interest from the standpoint of practical applications of the field cathodes, and has also been discussed in the literature.[11]

Finally, electrostatic forces predominate when the electric field $F$ at the emitter tip exceeds the value:

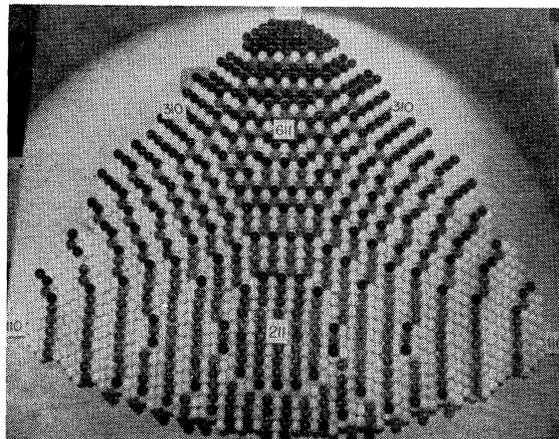$$F_0 \cong (16\pi\gamma/r)^{\frac{1}{2}}, \tag{1}$$



FIG. 1. "Marbles-for-atoms" model of a portion of a hemispherical field emitter with body-centered cubic crystal structure; surface radius of 50 atoms is about one-twentieth that of a typical emitter.

[3] E. W. Muller, Z. Physik 126, 642 (1949).

[4] W. P. Dyke and W. W. Dolan, Advances in Electronics and Electron Phys. 8, 89 (1956).

[5] J. K. Trolan, J. P. Barbour, E. E. Martin, and W. P. Dyke, Phys. Rev. 100, 1646 (1955).

[6] J. P. Barbour, F. M. Charbonnier, W. W. Dolan, W. P. Dyke, E. E. Martin, and J. K. Trolan, Phys. Rev. 117, 1452 (1960).

[7] I. L. Sokolskaya, J. Tech. Phys. (U.S.S.R.) 26, 1177 (1956) [translation: Soviet Phys. (Tech. Phys.) 1, 1147 (1956)].

[8] C. Herring, in Structure and Properties of Solid Surfaces, edited by R. Gomer and C. S. Smith (University of Chicago Press, Chicago, Illinois, 1953), p. 5; also in The Physics of Powder Metallurgy, edited by W. E. Kingston (McGraw-Hill Book Company, Inc., New York, 1951), p. 143.

[9] C. Herring, J. Appl. Phys. 21, 301 (1950).

[10] J. L. Boling and W. W. Dolan, J. Appl. Phys. 29, 556 (1958).

[11] W. P. Dyke, F. M. Charbonnier, R. W. Strayer, R. L. Floyd, J. P. Barbour, and J. K. Trolan, J. Appl. Phys. 31, 790 (1960).

where $r$ is the emitter tip in cm, and $F_0$ is in electrostatic units. In this case, with which the present paper is concerned, surface migration results in local rearrangements of the tip surface and also in a net flow of atoms from the emitter shank toward the tip, both of which contribute to the build-up process.

In the case of large applied fields a theoretical treatment is greatly complicated because the anisotropy of the crystalline cathode material has a preponderant effect on the geometrical changes which occur. By analogy with the low field case one might expect the heated emitter to grow in length when the applied field exceeds $F_0$; however, simple extension does not occur because of the very low probability of nucleating new atom layers in certain crystallographic plane orientations [such as (110), and to a lesser extent (100) and (211), in the case of body-centered cubic crystals] corresponding to relatively smooth surfaces. This low probability inhibits crystal growth in the corresponding directions, and as a result the heated field emitter does not remain smoothly rounded when subjected to fields greater than $F_0$, but builds up into a polyhedral shape in which the tip surface eventually consists of large plane facets separated by sharp edges and corners. The emitters used in this study were all made of tungsten wire with a [110] crystallographic direction parallel to the emitter axis, and the electric field at the emitter apex was at least twice $F_0$, resulting in a strong predominance of the electrostatic forces leading to build-up.

It will be recognized, from the marble-for-atom model of a tungsten field emission tip shown in Fig. 1, that small plane facets exist on an atomic scale for even the most smoothly rounded tip; the size of these facets, even though it remains small compared to the tip radius, is further increased because of the small anisotropy in the surface tension of tungsten. The initial stages of the build-up process are believed to consist essentially of a
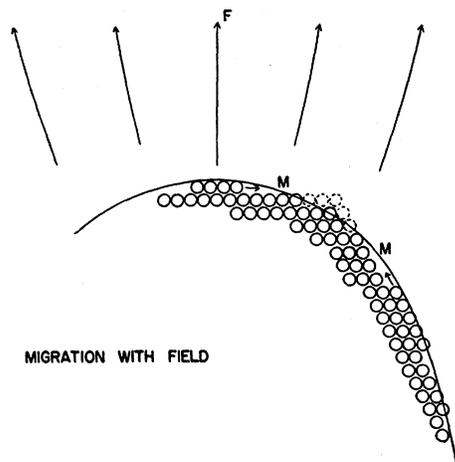
FIG. 2. Suggested mechanism of migration in the build-up process. Atoms from the low index planes are deposited in intermediate regions. Motion is toward the regions of higher field, i.e., greater curvature.
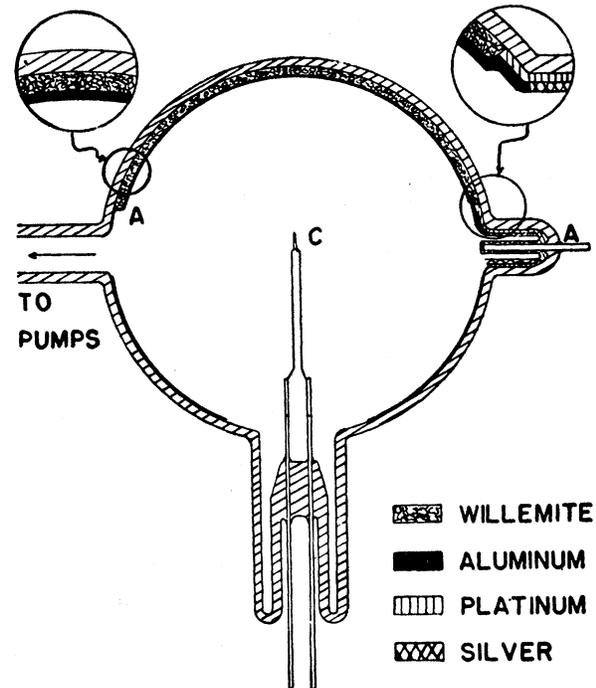
FIG. 3. Schematic drawing of the projection microscope field emission tube. $A$—anode; $C$—field emission cathode.

local rearrangement of atoms, as illustrated in Fig. 2; here we see that since the local fields are largest in the regions of greatest curvature, i.e., between the low index planes, the migration will be toward these regions, leading to some enlargement of the plane facets. This local migration is accompanied and followed by a slower transport of material from the emitter shank toward the apex, which gradually leads to the completely built-up form.

Two sets of experiments have been performed. In the first, the variable parameter was the tip temperature, while the tip radius $r$ and the initial electric field $F$ at the emitter apex were held constant, and the time interval $t$ required to evolve from one to another characteristic degree of build-up was determined as a function of temperature. Since this time interval is inversely proportional to the migration rate, the theory predicts a relationship of the form[11]:

$$t = CT \exp(Q_F/kT), \qquad (2)$$

where $C$ depends on the initial and final degrees of build-up selected for the measurement but is otherwise constant under the conditions of the experiment (constant $r$ and $F$), and $Q_F$ is the activation energy for the corresponding stage of the build-up process; thus a plot of $\ln(t/T)$ vs $1/kT$ would be expected to yield a straight line whose slope measures the activation energy $Q_F$.

In the second series of experiments the variable parameter was the initial electric field $F_0$ applied at the emitter apex, while the tip radius and temperature were
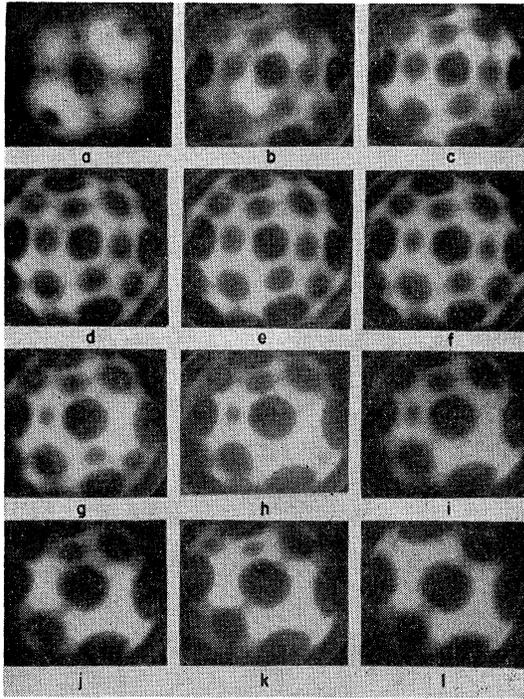
FIG. 4. Typical sequence of emission patterns for (211) build-up. $T=1800°K$, $r=4\times10^{-5}$ cm, $V=8000$ volts.

held constant. The dependence on $F$ of the characteristic build-up time $t$ was measured, and the theory was then used to determine the field dependence of the activation energy, as discussed in a later section.

### III. EXPERIMENTAL METHOD

Projection microscope tubes, of the type shown in Fig. 3, were used in the initial stages of the work. Their fabrication and evacuation, to pressures of the order of $10^{-12}$ mm Hg, have been discussed in the literature.[12,13] Electrons diverge from the field cathode $C$ and impinge on the metal backed phosphor coating which serves as the anode. The emission pattern as observed on the phosphor screen reveals an electron density distribution which is characteristic of the crystal structure and the geometry of the cathode surface. The magnitude of the current density depends on the work function and the shape of the surface and changes in those parameters are easily observed.

The emitter was heated by conduction from a resistively heated support filament. The temperature of each emitter was carefully calibrated as a function of filament current by use of an optical pyrometer, and the temperature was held constant during an experimental run. Correction was made for the calculated temperature drop due to radiation along the emitter shank.

[12] W. P. Dyke, J. K. Trolan, W. W. Dolan, and George Barnes, J. Appl. Phys. 24, 570 (1953).
[13] W. P. Dyke, J. K. Trolan, E. E. Martin, and J. P. Barbour, Phys. Rev. 91, 1043 (1953).

To observe build-up, the temperature of the emitter was set to a desired value and the electric field was then applied. The emission current was monitored on a chart recorder, and photographs of the emission patterns were taken as significant changes occurred.

Two distinctly different sequences of pattern changes were observed during build-up of the [110] oriented tungsten emitter. These are illustrated in Figs. 4 and 5. The two sequences differ significantly only in the latter stages of build-up when the (211) crystal regions "fill-in" in the first case and the (100) crystal regions fill-in in the second. The corresponding respective emission currents are shown in Figs. 6 and 7; correlation of the patterns with time and the emission current are indicated on the curves. It is to be noted that an initial rapid change in the patterns and current is followed by a relatively quiescent stage during which little change is observed; only a general growth in the large dark areas representing the low index (100), (110), and (211) planes of the crystal surface is noted. Finally there follows a rapid sequence of events in which certain of the dark areas fill in and brighten, accompanied by large increases in the current. The current then levels off to a somewhat unstable value and the patterns cease to change. Continued operation at this level usually results in destruction of the tip through vacuum arc.[14] This would be expected since the local current density in the build-up regions is very high (of the order of $10^8$ amp/cm²) and would lead to resistive heating of the emitter tip.[13]
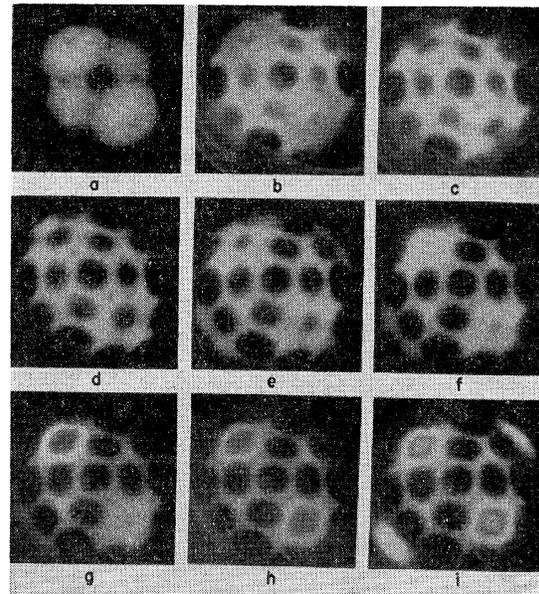


FIG. 5. Typical sequence of emission patterns for (100) build-up. $T=1800°K$, $r=4.1\times10^{-5}$ cm, $V=8070$ volts. Dark areas in center of (100) regions of patterns g, h, i are caused by intense electron current heating phosphor and destroying fluorescent property.

[14] W. W. Dolan, W. P. Dyke, and J. K. Trolan, Phys. Rev. 91, 1054 (1953).

Shadow micrographs of the emitter tips before and after build-up illustrate the changes from the smoothly rounded to the polyhedral form as shown in Figs. 8 and 9 for "211" and "100" build-up, respectively. The middle and right-hand profiles in each figure correspond to two different orientations of the emitter. These orientations are indicated on the appropriate pattern pictures of Figs. 8-B and 9-B. The polyhedral angles appearing in the profiles of the build-up emitters were measured and compared with the calculated values for the body-centered cubic crystal structure of tungsten. Very close agreement was obtained.

The built-up emitter can be restored to its initial smooth form by flashing to a high temperature (about 2700°K) for a short period. Build-up can then be repeated at the same or a different temperature and an essentially identical sequence of patterns and currents is observed; however, the rate of build-up is highly de-
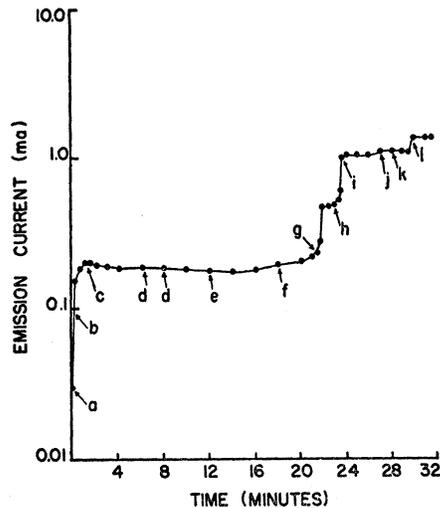


FIG. 6. Typical emission current change for (211) build-up. Letters indicate corresponding patterns of Fig. 4.

pendent on the temperature. This is especially true for the initial period of the build-up process and provides the method for obtaining the activation energy $Q$.

The projection microscope tube was used in the early stages of the experimental work since the ability to view the emission patterns and thereby follow the changes in the emitter geometry was invaluable in the establishment of the current-geometry relationship and the interpretation of the results. However, it was recognized that in this type of tube the inability to outgas completely surfaces on which the electrons impinged could lead to liberation of surface gases and to ion bombardment and contamination of the emitter during operation. It was felt that these effects might have some effect on the migration rate. After experience was gained through extensive operation, it was found that the build-up process could be followed through monitoring the emission current alone. This allowed the substitution of a tung-
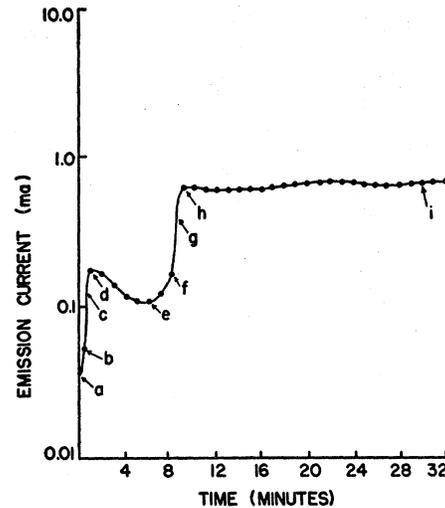


FIG. 7. Typical emission current change for (100) build-up. Letters indicate corresponding patterns of Fig. 5.

sten anode which could be thoroughly outgassed during evacuation. The latter tube is illustrated in Fig. 10. The tungsten anode almost completely surrounds the emitter and effectively traps the primary and secondary electrons, keeping them from bombarding the poorly outgassed portions of the tubes. In addition these tubes were made of Corning No. 1720 glass which is relatively impervious to the infusion of helium from the atmosphere.[15] Tests showed that these tubes could be operated cold at a high dc current level for many hours
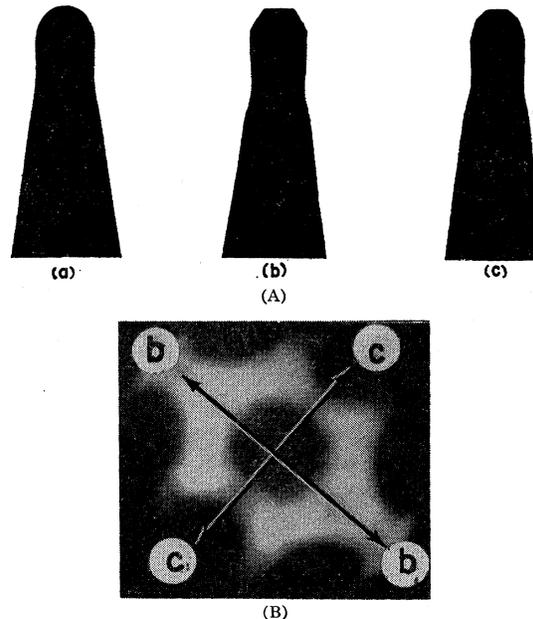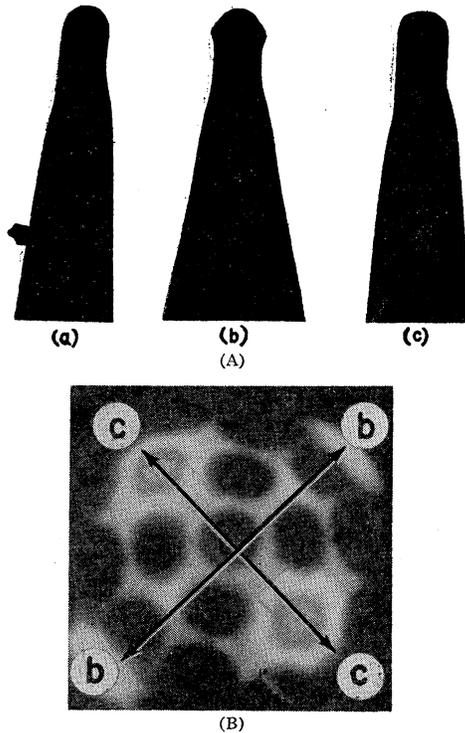


FIG. 8. Electron micrograph profiles of emitter before and after (211) build-up. Insert shows orientation of build-up profiles with respect to emitter patterns.

[15] F. J. Norton, J. Am. Ceram. Soc. 36, 90 (1953).

FIG. 9. Electron micrograph profiles of emitter before and after (100) build-up. Insert shows orientation of build-up profiles with respect to emitter patterns.

with no appreciable deterioration of the field cathode, and from this it is concluded that contamination and ion bombardment rates were negligible.

From the discussion given above it is evident that there exists a very close correspondence between the changes in the emission patterns and changes in the emission current during build-up. Similar points on each of a family of current curves for which temperature is the variable parameter can be identified and are assumed to correspond to the same degree of build-up. The temperature dependence of the rate of build-up is thus obtained and the activation energy $Q$ derived through the use of Eq. (2). Figure 11 represents a typical set of curves. The points labeled $k, k, \ldots, k$ represent the same stage in the build-up process. The corresponding values of temperature and time are presented as points of Fig. 12. The slope of the line determines a value of $Q$. Other sets of points such as $a, a, \ldots,$ $b, b, \ldots, b$, etc., could have been selected. However,

TABLE I. Summary of mean values for $Q$(ev/atom).

| Emitter No. | Mean for each emitter | Mean for type of anode |
|---|---|---|
| W2A415 \\ W2A418 ⎱—Phosphor Anode | 2.34±0.08 \\ 2.29±0.06 | 2.31±0.07 ($Q_P$) |
| W2A642 \\ W2A643 ⎱—Tungsten Anode | 2.46±0.04 \\ 2.42±0.06 | 2.44±0.05 ($Q_T$) |

those indicated by $k$ were preferred for the following reasons: (1) they represent the most prominent identifiable feature, the knee of the curve where it levels off after the first large increase in current; (2) the prominent knees correspond to the emission patterns of Fig. 4(c) and Fig. 5(d) and occur fairly early in the build-up process, so that they do not represent a large departure from the initial rounded form of the emitter tip. Therefore, conditions are more likely to be the same for each repetition of the process than at some later time, and Eq. (2) can be used with confidence. At earlier times a well defined break or inflection is often lacking.

## IV. EXPERIMENTAL RESULTS

The mean values of $Q$ and the statistical probable errors are given in Table I. These have been grouped according to the type of anode and tube used.

The difference in the values of $Q$ as obtained from the two types of tubes is significant since a calculation of $\sigma_d$, the standard deviation of the difference between the two values, gives

$$\sigma_d = 0.04.$$

The difference in $Q$ is

$$Q_T - Q_P = 0.13 \approx 3\sigma_d.$$

As has been suggested previously, the larger value of $Q$ obtained in the tungsten anode type of tube is believed due to the better environmental conditions which alleviate ion bombardment and the resulting excitation of the surface atoms of the emitter tip during operation.
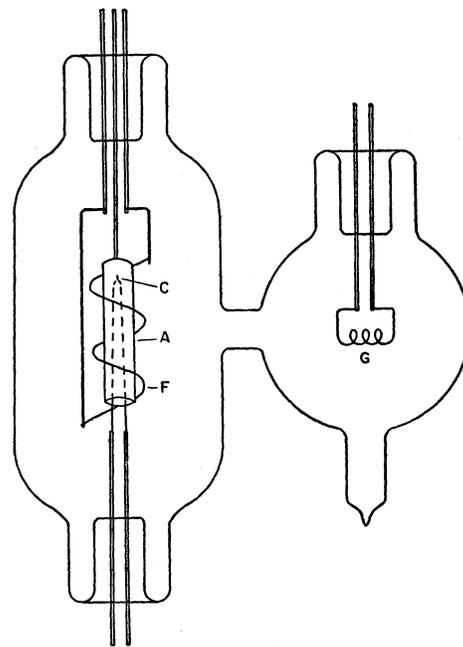


FIG. 10. Schematic drawing of tungsten anode field emission tube. A—anode cup, C—field emission cathode.

For this reason the larger value of

$$Q = 2.44 \pm 0.05 \text{ ev/atom}$$

is believed to be the more acceptable value.

A résumé of the results of other investigators has been given in the introduction. Their quoted values for the activation energy for surface migration are summarized in Table II for convenience.

The values obtained for the activation energy fall into two groups, depending on the direction of the net migration. The values within each group are consistent within the accuracy of the measurements. However, the difference of about 30% between the two sets of values is well outside the respective experimental uncertainties and requires explanation.

An obvious factor contributing to this difference is the fact that a large electric field is present at the

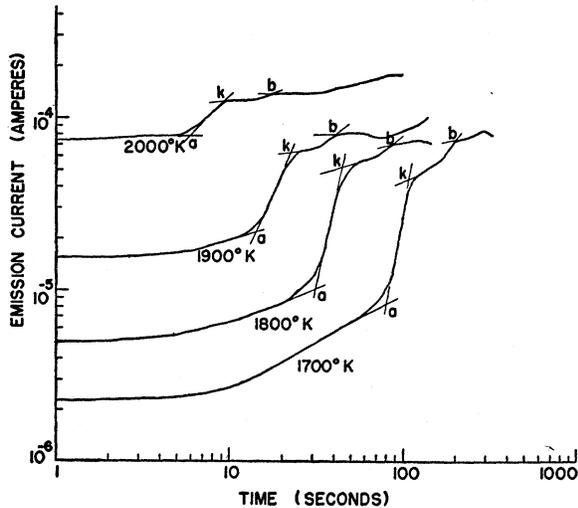FIG. 12. Plots of log $t/T$ vs $10^4/T$ for data from curves of FIG. 11. Slope of line equals $Q/R$.

FIG. 11. Typical family of build-up current curves for constant applied potential $V = 6960$ volts.

emitter surface in the case of the build-up experiments, and the activation energy is expected to vary with applied field as pointed out by Drechsler.[16] A quantitative estimate of this effect is a prerequisite to a meaningful comparison of the two sets of value. The experimental data gives no clear evidence of a change of $Q$ with applied field. However, because of the small range of field accessible to the experiment, the small corresponding variation in $Q$ may well be masked by the spread in experimental measurements.[17] In order to elucidate

this point, the following analysis and experiment were performed.

## V. FIELD DEPENDENCE OF THE ACTIVATION ENERGY

As noted earlier, the data used for the determination of the activation energy was restricted to the early stages of the build-up process, during which the emitter departs from its well-known initial shape by a small amount only. Under those conditions it is permissible to use the initial emitter profile, obtained by electron microscope shadowgraphs as illustrated in Fig. 8(a), to determine at the tip surface the curvature and field distributions which are needed for the determination of the surface migration constants by means of Eq. (2). The functional dependence of the characteristic build-up times $t$ on the essential parameters (tip radius $r$, applied electric field $F$ at the emitter apex, and tip temperature $T$) may thus be obtained,[11] leading to the expression:

$$t = C r^3 \frac{T \exp Q_F/kT}{F^2 - F_0^2}, \qquad (3)$$

where $C$ is a constant depending on the initial and final degrees of build-up selected for a specific measurement, and $F_0$ is the minimum field required to produce build-up and given in Eq. (1).

According to Drechsler[16] the effect of an external electric field is to induce an electric dipole in an atom

FIG. 13. Schematic representation of the field at a metal surface on microscopic scale.

---

[16] M. Drechsler, Z. Elektrochem. **61**, 48 (1957).

[17] Electrostatic stresses at the crystal surface are proportional to $F^2$. Therefore, as confirmed experimentally, the effect of an external electric field on the surface migration and build-up rates depends on the magnitude of the field but not on its polarity. However, in the present experiments the emitter tip was made cathodic to permit monitoring of the build-up process through the field emission current and pattern, and only a narrow range of applied fields could be used satisfactorily because of the very sensitive dependence on field of the field emitted current.
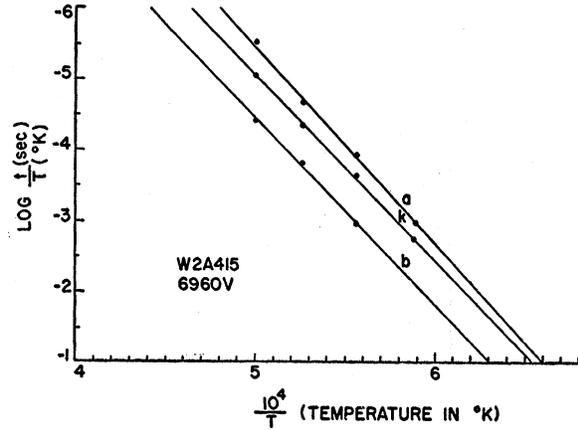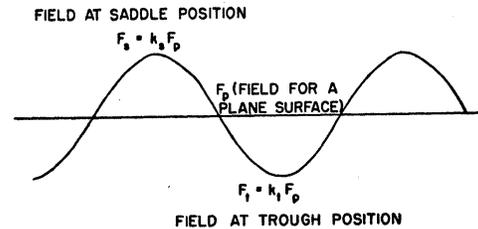
TABLE II. Measured values of activation energy for the surface migration of tungsten on its own lattice.

| | Author | Date | Activation energy in ev/atom | Direction of migration | Temperature range |
|---|---|---|---|---|---|
| Group I | Müller | 1949 | 3.5±0.3 | Dulling (no applied field) | 1200°K to 1500°K |
| | Sokolskaya | 1956 | 3.2±0.2 | Dulling (no applied field) | 1200°K to 1600°K |
| | Barbour et al. | 1959 | 3.14±0.08 | Dulling (no applied field) | 1800°K to 2700°K |
| Group II | Sokolskaya | 1956 | 2.36±0.2 | Build-up (large applied field) | 1200°K to 1600°K |
| | Present work | | 2.44±0.05 | Build-up (large applied field) | 1700°K to 2100°K |

migrating on the surface, which results in an additional binding energy $E_F$ given by:

$$E_F = \tfrac{1}{2}\alpha F^2, \tag{4}$$

where $\alpha$ is the polarizability coefficient. If we take into account the atomic structure of the emitter tip, the surface field may be represented as illustrated in Fig. 13 where $F_p$ is the field corresponding to an ideally smooth surface, $F_t = k_t F_p$ is the field at a stable site for the migrating atom ($k_t < 1$) and $F_s = k_s F_p$ is the field at the potential saddle which the atom must cross when migrating from a stable site to the next ($k_s > 1$). It follows that the activation energy for surface migration, which is the difference between the binding energies of the migrating atom at the trough and saddle positions, will decrease with increasing field according to the expression:

$$Q_F = Q_1 - \tfrac{1}{2}\alpha(k_s^2 - k_t^2)F_p^2 \equiv Q_1 - AF_p^2, \tag{5}$$

where $Q_F$ is the activation energy measured in the presence of field and $Q_1$ is the activation energy corrected for the field effect (i.e., $Q_1$ rather than $Q_F$ should be compared to the activation energy $Q_0$ measured in the dulling experiments of Table II, group I).

Substituting Eq. (5) into Eq. (3) yields:

$$t = Cr^3 \frac{T \exp[(Q_1 - AF^2)/kT]}{F^2 - F_0^2}. \tag{6}$$

Taking the natural logarithm of both sides of Eq. (6) and differentiating with respect to F, one obtains:

$$d(\ln t) = -nd(\ln F), \quad \text{where} \quad n = 2AF^2/kT$$
$$+2F^2/(F^2 - F_0^2), \tag{7}$$

and finally, in view of Eq. (5):

$$Q_1 = Q_F + kT\left[\frac{n}{2} - \frac{F^2}{(F^2 - F_0^2)}\right]. \tag{8}$$

This expression allows calculation of $Q_1$ from the experimental data, since $F_0$ is given by equation (1) and since $n$ is a directly measurable quantity equal to the slope of the curve $t(F)$ plotted in logarithmic coordi-

nates. It will be noted that, whereas the value of the constant $A$ depends on the detailed atomic structure of the surface, through the coefficients $k_t$ and $k_s$, the final Eq. (8) for $Q_1$ does not require knowledge of these quantities, and its validity requires only that the field dependent term of $Q$ be proportional to the square of $F$.

Experimental values of $n$ were obtained for emitters W2A642 and W2A643 by observing the field dependence of the build-up time at constant temperature. A typical set of time versus current curves for this test is given in Fig. 14, and the corresponding $\ln t$ vs $\ln F$ curves are shown in Fig. 15. The mean of six experimental determinations yields:

$$n = 7.5 \pm 0.24,$$

where $\pm 0.24$ represents the probable error corresponding to the statistical scatter of the measurements. Substituting into Eq. (8), the reference value
$Q_1 = (2.44 \pm 0.05) + (0.35 \pm 0.06) = 2.79 \pm 0.08$ ev/atom
is obtained for the activation energy for build-up of tungsten emitter tips, after correction has been made for field effect.
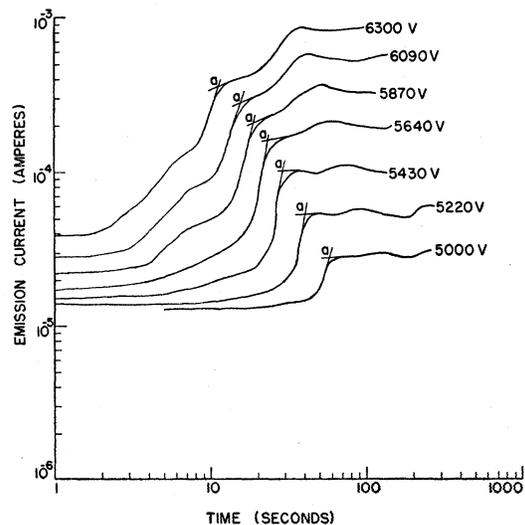


FIG. 14. Typical family of build-up current curves for constant temperature. Applied potential is the variable parameter.

## VI. DISCUSSION OF RESULTS AND CONCLUSIONS

The diffusion theory developed by Herring[7] has been utilized to obtain an experimental value of the activation energy of surface migration in the presence of electric field (build-up) on the heated tungsten field emission tip. The work has yielded a value ($Q_F = 2.44 \pm 0.05$ ev/atom), calculated from the experimental data, which is considerably lower than that obtained by other workers from the dulling rate of a smoothly rounded, heated emitter when no field is applied ($Q_0 \cong 3.14 \pm 0.08$ ev/atom). Considerations of the possible effects of field on the migration rate and of the atomic structure of the tungsten crystal, and observation of the build-up process in the field emission microscope have led to proposal of the following mechanisms to explain the difference.

The high electrostatic field present at the crystal surface during build-up causes, through induced polarization of the surface atoms, a reduction of the potential hill which an atom must surmount in order to migrate from one stable site to another. One should therefore expect a variation of $Q$ with applied field; however, in the initial experiment the range of fields which could be used was too small to give conclusive evidence of this variation. An auxiliary experiment has yielded an experimental determination of the field effect, which leads to an adjusted value of $Q_1 = 2.79 \pm 0.08$ ev/atom for the activation energy of the build-up process referred to zero applied field.

This value of $Q_1$ is directly comparable to the value of $Q_0 = 3.14 \pm 0.08$ ev/atom found for the dulling process. The difference is statistically significant, and since it cannot be ascribed to field effects it shows that build-up is not simply a reverse of the dulling process, i.e., build-up is not due entirely to material migrating from the emitter shank toward the tip. An explanation of this difference is proposed, based on the study of the physical processes involved and supported by experimental evidence. Observations of the growth in size of the dark (100), (110), and (211) areas of the tungsten field emission pattern during the early stages of build-up have suggested that the predominant change in the emitter during this initial period results from the migration of atoms outward from the center area of these regions, producing an extension of these low index planes and a deposition of atoms at the intermediate regions. The consideration of the local action of the fields at the emitter tip and the study of electron micrograph profiles of the emitter tip after build-up, as well as current studies of emitter tips containing screw dislocations, have further supported and corroborated this view.

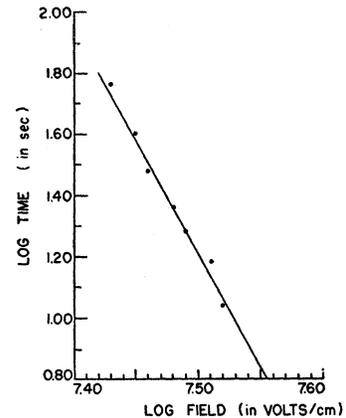It is difficult to give a detailed evaluation on an



FIG. 15. Plot of data from Fig. 14. Slope of line = $n$.

atomic scale of the energy required to achieve migration at all specific surface lattice sites. However, because of the relative smoothness and lack of deep potential traps on the (110), (100), and to a certain extent (211) planes, compared to other regions of the emitter tip surface, migration over these regions is expected to proceed more easily, yielding a relatively low value of activation energy. On the other hand, the activation energy as measured for the emitter dulling process involves a gross transport of atoms from the apex of the emitter toward the shank; the migration thus takes place to a large extent over a rougher surface, and a correspondingly greater value of activation energy is to be expected.[6]

Thus it is concluded that, in its early stages, the build-up process results primarily from local rearrangements of the tip surface in which the large applied electric field causes the atoms in the uppermost layers of the initially small (110), (100), and (211) plane facets to accumulate by surface migration at the outer edges of these facets, and that the lower activation energy associated with this local migration accounts for the difference between the activation energies measured for the build-up and dulling processes which remains after allowance has been made for the variation of activation energy with field. Preliminary observations suggest, however, that surface migration from the emitter shank predominates in the later stages leading to complete build-up.
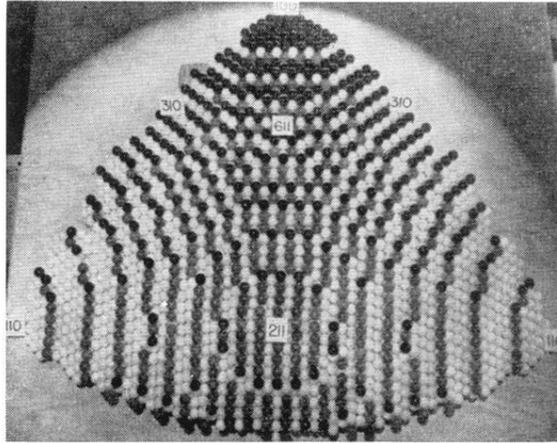
### ACKNOWLEDGMENTS

Fig. 1. "Marbles-for-atoms" model of a portion of a hemi-spherical field emitter with body-centered cubic crystal structure; surface radius of 50 atoms is about one-twentieth that of a typical emitter.
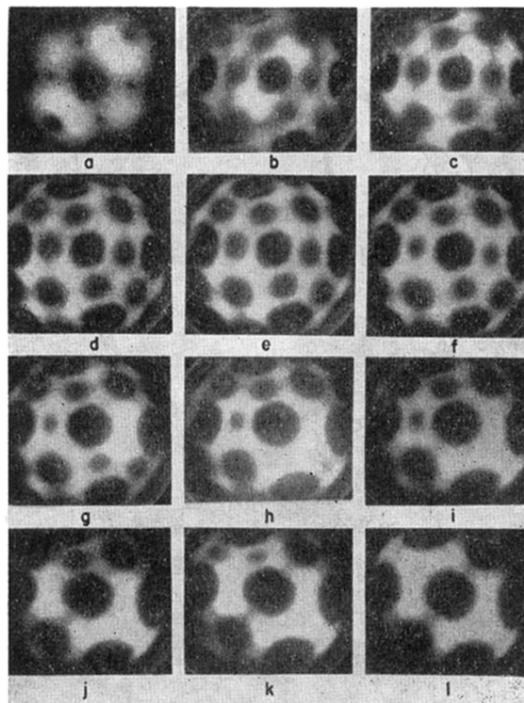
FIG. 4. Typical sequence of emission patterns for (211) build-up. $T = 1800°$K, $r = 4 \times 10^{-5}$ cm, $V = 8000$ volts.
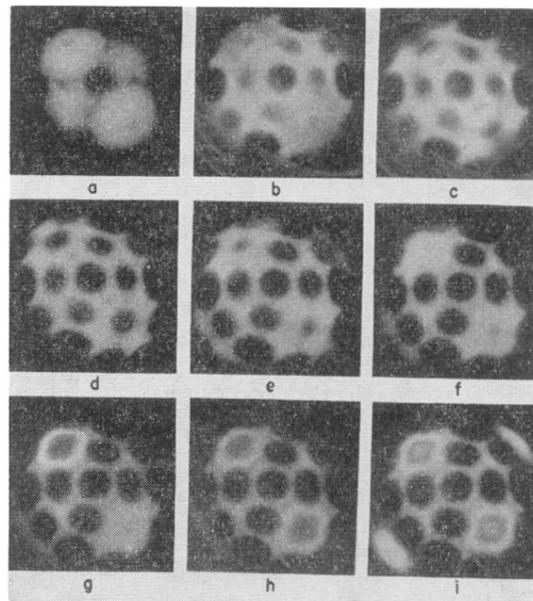
Fig. 5. Typical sequence of emission patterns for (100) build-up. $T = 1800°K$, $r = 4.1 \times 10^{-5}$ cm, $V = 8070$ volts. Dark areas in center of (100) regions of patterns $g$, $h$, $i$ are caused by intense electron current heating phosphor and destroying fluorescent property.
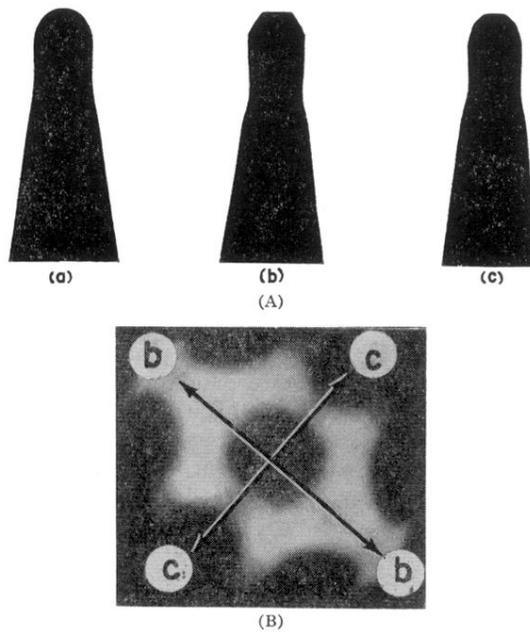
(A)

(B)

Fig. 8. Electron micrograph profiles of emitter before and after (211) build-up. Insert shows orientation of build-up profiles with respect to emitter patterns.
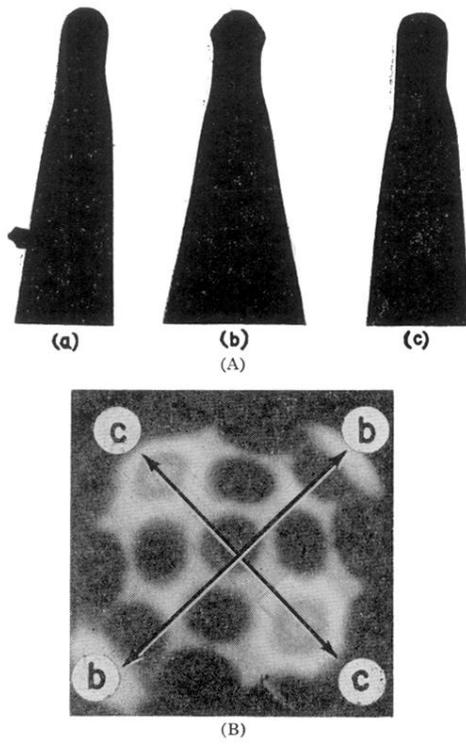
(a)    (b)    (c)

(A)

(B)

Fig. 9. Electron micrograph profiles of emitter before and after (100) build-up. Insert shows orientation of build-up profiles with respect to emitter patterns.